Chapter 1

Introduction

Complex (dusty) plasma is a multicomponent plasma containing electrons, ions, dust particles and neutrals. Complex plasmas contain dust particles that interact with the surrounding plasma by absorbing electron and ion fluxes. This interaction necessitates external source of energy and plasma particles to compensate for the loss of energy and matter. The presence of dissipation of energy and thermodynamic openness lead to many self-organization phenomena in complex plasmas. In this introductory chapter, some basic properties of complex plasma are described besides discussing the occurences of complex plasma both in terrestrial laboratories and space environments. Some examples of self-organization phenomena are also explored in this chapter. In addition, systems of small number of charged dust particles can be formed in complex plasmas, where these small clusters of charged dust particles are referred to as Yukawa clusters. Finite systems consisting of a small number of charged particles occurs in many other physical systems like, ions in traps, electrons above the surface of liquid He and electrons in quantum dots etc. Hence, these Yukawa clusters serve as model systems to study finite systems with the added advantage that the particle dynamics can be studied at individual kinetic level due to large size and mass of the dust particles. In this chapter, some introductory remarks about these finite clusters in the absence and presence of an external magnetic field have been made which will be developed further in the later chapters.

1.1 Complex plasma as a branch of plasma physics

Plasma is considered the fourth state of matter. It is said that almost 99% of the visible Universe is in the plasma state. Plasma occurs in nature in different environments like in the Sun, in white dwarf and neutron stars, in Earth's upper atmosphere etc. The term plasma was first coined by I. Langmuir in 1929 to denote a region of gas discharge with nearly equal electron and positive ion densities [1, 2]. Plasmas exhibit both collective and single particle behaviour depending upon the length scale under consideration (i.e, for $k << K_D$ the plasma behaves as a medium whereas for $k >> K_D$ the individual particle motions becomes dominant where, k and K_D are respectively the wavenumber and inverse Debye length) [3]. Collective phenomena in plasma include Debye shielding, plasma oscillation, various kinds of waves etc. The collective behaiviour in plasma arises because of the long-range nature of the interaction potential among the particles. The number of particles in a Debye sphere has to be much larger than unity in order for collective effects to play dominating role over binary collisions. Plasmas are studied extensively in different laboratories around the world. Many basic plasma phenomena are of interest to physicists.

Complex (dusty) plasma is a branch of plasma physics which deals with a system of micron or sub-micron sized particulates immersed in an electron-ion plasma. These particulates get charged by collecting electrons and ions from the surrounding plasma and they can charge both positively as well as negatively. The problem of dusts immersed in plasmas historically occured in space plasmas and not in laboratory plasmas. Dusty plasmas are found in planetary rings, interstellar medium, cometrary tails etc. Dusty plasma is a suitable model system to study phenomena resulting from strong correlation among the particles. Strong correlation can be achieved at room temperature in dusty plasma because the grains charge upto several thousands of electronic charges. The grains charge mainly by collecting electrons and ions onto their surfaces. The emission of secondary electrons and photoemmision also contribute towards particle charging [4, 5]. A brief description of particle charging in dusty plasmas is given in section 1.3. The particle charge in a complex plasm varies in both space and time which makes it a fundamentally different from an ordinary many body system consisting of

elementary particles having fixed charges.

The interaction among the dust grains in dusty plasmas can be both collective as well as non-collective. In a large homogeneous dusty plasma (in principle an infinite complex plasma) containing a large number of particles the interaction among the grains can be considered collective as it depends upon the average dust density and average charge on the particles. But in an inhomogeneous dusty plasma the intergrain interaction generally doesn't depend on the average values of parameters and hence the interaction becomes non-collective. For collective interactions to govern the behaviour of the system of grains, the system size has to be much larger than the mean free path of ion-grain interaction [6] so that the ion fluxes onto different grains can interfere.

Complex plasma can be understood as an instance of soft-matter. Soft matter is the class of matter which shows macroscopic softness, metastable states and is sensitive to external conditions at equilibrium [7]. Due to the presence of ion flow, anisotropic interactions may arise in complex plasma in the form of attractive wake potential among the grains. It has been shown that the presence of an external magnetic field and ion-flow gives rise to tunable attractive wake potential which makes it possible to use complex plasma in studying magneto-rheological characteristics of soft matter [8]. Besides magneto-rheological characteristics the electro-rheological characteristics also can be tuned by tuning the ion cloud surrounding a dust grain to any shape by adjusting an external electric field [9]. Complex plasma qualifies to be considered as a non-Hamiltonian system because of the variation of dust charge. The energy of particle ensemble is not conserved during interparticle collsions [10].

The study of complex plasma phenomena is relevant to some biological systems also. For example, the melting criterion developed for complex plasma crystals can be used for biological crystals [11], pattern formation studies in magnetic fields can be relevant for biological systems etc. [12].

1.2 Key properties of dusty plasma

1.2.1 Macroscopic neutrality

As it is found in electron-ion plasma, dusty plasma also exhibits macroscopic neutrality. In equilibrium, and in the absence of any external force, the dusty plasma is macroscopically neutral. The presence of dust particles in plasmas can reduce electron density as the electron flux on to the dust particles is more than the ion flux. So, the electron density depletes more in comparison to ion density. The macroscopic neutrality condition by considering negatively charged dust particles, electrons and positively charged ions is expressed as,

$$q_d n_d + e n_e = q_i n_i. \tag{1.1}$$

In the above, q_d, e and q_i are dust charge, electronic charge and ion charge respectively and n_d, n_e and n_i are number densities of dust, electrons and ions respectively.

1.2.2 Debye Shielding

When a charged object is injected into a plasma, the oppositely charged particles shield the electric field of the charged object. This gives rise to a spherical cloud of finite radius surrounding the charged object. The particles lying at the edge of the cloud feels less potential energy and hence is affected more by the thermal agitation. The radius of the cloud is hence decided by the competition between the potential and kinetic energies of the particles at finite non-zero temperature.

In the linear approximation, the Debye length for the dusts can be expressed as,

$$\lambda_D = \frac{\lambda_{De}\lambda_{Di}}{\sqrt{\lambda_{De}^2 + \lambda_{Di}^2}}, \tag{1.2}$$

where, $\lambda_{De} = \sqrt{k_B T_e / 4\pi n_e e^2}$ and $\lambda_{Di} = \sqrt{k_B T_i / 4\pi n_i e^2}$ are the electron and ion Debye lengths respectively. Here, $n_{e(i)}$, e and $T_e(i)$ are respectively electron(ion) density, electronic charge, and electron(ion) temperature respectively. For a dusty plasma with negatively charged dust grains electron density becomes much less than ion density and electron temperature becomes much higher than ion temperature and so $\lambda_{De} >> \lambda_{Di}$ which leads to $\lambda_D \sim \lambda_{Di}$.

1.2.3 Characteristic frequencies

When a plasma is perturbed, the local space charge field developed can make a charged particle oscillate around its equilibrium position. The oscillation frequency depends upon the charge to mass ratio of the plasma specie. In general, the oscillation frequency is expressed as, $\omega_{ps} = \sqrt{4\pi n_{0s} q_s^2/\epsilon_0 m_s}$, $s \in \{i, e, d\}$. Here, i, e and d denote respectively the ions, electrons and dusts. Besides plasma oscillation the plasma species also suffer from collision with the neutrals. The collision with the neutrals tends to damp the collective oscillations and gradually diminish their amplitudes [4].

1.2.4 Coulomb coupling parameter

For a One Component Plasma(OCP) the particles interact among themselves via pure Coulomb repulsion. Such a system can be characterized by the ratio of average interparticle potential energy to the average thermal energy known as a Coulomb coupling parameter and defined as $\Gamma = \frac{q_d^2}{4\pi\epsilon_0 r_{av} k_B T_d}$. For a system of particles with large particle charge and low kinetic temperature and smaller interparticle distance, the average interparticle potential energy of the particles can become much higher than the average thermal energy. In such a situation, Γ becomes much higher than unity. A plasma is called strongly coupled if $\Gamma >> 1$ and weakly coupled if $\Gamma << 1$.

In a dusty plasma, the field of the dust grains are screened due to the presence of a background plasma. The interaction among the dust grains therefore is modeled via screened Coulomb potential. In such a system an effective Coulomb coupling parameter can be defined as $\Gamma_{eff} = \Gamma \exp(-\kappa)$, where κ is called screening parameter and is defined as $\kappa = \frac{r_{av}}{\lambda_D}$, r_{av} being the mean interparticle distance. It was shown by Ikezi that for $\Gamma_{eff} > 168$ the dust grains can form crystalline pattern known as plasma crystal [13].

1.3 Particle charging in dusty plasma

To understand the charging of the dust grains in plasma the Orbital Motion Limited (OML) approach is used. Some assumptions used in the OML approach are [14],

1) The dust grain is isolated so that the electrons and ions surrounding a dust grain are not affected by other dust grains,

2) Electrons and ions don't suffer collision with the neutrals,

3) The barriers in effective potential are absent.

The ion current onto the surface of a dust particle of radius a is obtained as,

$$I_i = \pi r_d^2 n_i e \sqrt{\frac{8k_B T_i}{\pi m_i}} \Big(1 - \frac{e\phi_p}{k_B T_i}\Big), \tag{1.3}$$

In the above expression, ϕ_p denotes the potential due to a dust grain, m_i is the ion mass and r_d is the radius of a dust particle. This can be seen as the product of ion current density given by $j_i = n_i e\sqrt{\frac{8k_B T_i}{\pi m_i}}$ and an effective crossection of collection of ions onto a dust grain given by, $\sigma = \pi r_d^2\Big(1 - \frac{e\phi_p}{k_B T_i}\Big)$ [15]. Similarly, the electron current is obtained as,

$$I_e = -\pi r_d^2 n_e e \sqrt{\frac{8k_B T_e}{\pi m_e}} \exp\Big(\frac{e\phi_p}{k_B T_e}\Big), \tag{1.4}$$

where, m_e is the electronic mass. The time evolution of dust charge can now be expressed as,

$$\frac{dq_d}{dt} = I_i + I_e. \tag{1.5}$$

The above expression for ion current hold for Maxwellian plasma. In the presence of streaming ions, the ion velocity distribution doesn't remain Maxwellian and in that case, the OML theory needs to be modified.

In the presence of ion flow and when the ion streaming speed is much higher than the ion thermal speed, the ion current can be expressed as [15],

$$I_i = \pi r_d^2 n_i e v_i \Big(1 - \frac{2e\phi_p}{m_i v_i^2}\Big), \tag{1.6}$$

where, v_i denotes the ion streaming speed. In equilibrium, the ion current becomes equal to the electron current. So, from Eq. 1.3 and 1.4,

$$\pi r_d^2 n_i e \sqrt{\frac{8k_B T_i}{\pi m_i}} \Big(1 - \frac{e\phi_p}{k_B T_i}\Big) = -\pi r_d^2 n_e e \sqrt{\frac{8k_B T_e}{\pi m_e}} \exp\Big(\frac{e\phi_p}{k_B T_e}\Big), \tag{1.7}$$

and it can be shown that in the limit of $e\phi_p << k_B T_e$ the dust surface potential becomes,

$$\phi_p = -\frac{k_B T_e}{e} \frac{1 + \sqrt{\frac{m_e T_i}{m_i T_e}}}{1 - \sqrt{\frac{m_e T_e n_i^2}{m_i T_i n_e^2}}}. \tag{1.8}$$

Now, considering the dust particle as a spherical capacitor with capacitance $C = 4\pi\epsilon_0 r_d$, the equilibrium dust charge can be written as,

$$q_d = C\phi_p = -\frac{4\pi\epsilon_0 r_d k_B T_e}{e} \frac{1 + \sqrt{\frac{m_e T_i}{m_i T_e}}}{1 - \sqrt{\frac{m_e T_e n_i^2}{m_i T_i n_e^2}}}. \tag{1.9}$$

There are also some other mechanisms by which a dust grain may charge up in a dusty plasma :

- **Photoelectric emission :** Dust particles can charge via emission of electrons by the photoelectric process. The incidence of photons having energy greater than the work function of the dust grain material leads to emission of electrons from dust surface therby making the dust grains positively charged. So, the photoelectric emission process gives rise to a positive charging current. The emission of electrons by this process depends upon the material of the dust grains, the wavelength of the incident light and surface area of the dust particles [4]. Charging of dust particles by photoelectric emission is relevant for astrophysical plasmas [15].

- **Thermionic emission :** Thermionic emission is a process where electrons are emitted from a body when heated as they get enough kinetic energy to leave the surface of the material. A dust grain can be heated by lasers, IR heating or by hot filaments [4] so that it emits electrons thereby charging the dust grain positively.

- **Secondary electron emission :** Dust particles also may charge up via emission of electrons due to incidence of highly energetic electrons or ions on the dust surface. The secondary electron emission may be significant if the energy of the incident particles are sufficiently higher. The yield of secondary electrons is defined as the ratio of the emitted electron flux to the incident electron flux. The yield depends strongly on the energy of the

incident electrons [16, 15]:

$$\delta(E) = 7.4\delta_M \frac{E}{E_M} \exp(-2\sqrt{(E/E_M)}), \tag{1.10}$$

where, δ_M is the maximum yield when $E = E_M$.

1.4 Occurence of dusty plasma

1.4.1 Dusty plasma in space

Dusty plasma occurs in different astrophysical environments. For example, it occurs in interstellar and circumstellar clouds [4], Supernovae and Supernovae remnants [17], Solar system and Earth's atmosphere etc. As these dust grains are charged and massive, their dynamics are controlled both by electromagnetic and gravitational force.

Dust grains play an important role in the physics of the interstellar medium. Interstellar medium (ISM) refers to the space between stars in a galaxy. The presence of dust in ISM was first ascertained by studies of extinction of starlight. The insterstellar dust is formed due to the condensation of heavier chemical elements like C, O, Mg, Si and Fe which are released in the ISM during the evolution of the stars. Although initially the studies of interstellar dust was motivated by the need to correct the spectra of reddening and extinction, now-a-days the studies of dust have become an important factor in understanding the thermodynamics and chemistry of the gas and dynamics of star formation [18]. Spitzer studied the processes by which a dust particle in interstellar medium acquires charge [19]. He showed that if the electron density of the interstellar medium becomes $10^{-3}\ cm^{-3}$ the dust particles get charged due to collision with the rapidly moving electrons rather than due to photoelectric ionizations.

Dusty plasma also occurs in the Earth's atmosphere. Earth's mesosphere is the region between 50 and 90 km above the Earth's surface. In the polar summer mesopause there occurs a special cloud known as the "Noctilucent Clouds" as shown in Fig. 1.1 lying between 80 and 90 km altitude. A population of the so called "smoke particles" exists in the upper parts of the mesosphere which

Figure 1.1: Noctilucent clouds over Stockholm. Photograph taken by Kevin Cho (`www.kevinchophotography.com`) and distributed under CC BY-SA 4.0 license, taken from Wikimedia Commons.

forms due to burning up of the meteor particles and subsequent re-condensation of the evaporated gas. Smoke particles consist of metal and silicate compounds and have radii of less than a few nanometers. During summer the temperature of the upper portion of the mesosphere called mesopause becomes 110-150 K. The water vapor in the mesopause condenses on the meteor particles to form icy dust particles which may be observed visually as Noctilucent Clouds (NLC) [5]. Another mesospheric phenomenon related to the dust particles is called Polar Mesospheric Summer Echoes (PMSEs). The density gradient in the charged dust (ice) particles which occurs due to neutral turbulence causes density gradients in the electron gas and this causes the radio waves to backscatter from the dust layers [5, 20].

Dust particles are found in the rings surrounding different planets of the solar system for example the rings of Jupiter and Saturn. Their dynamics is mainly determined by gravity, electromagnetic, drag and radiation pressure forces. The surface potential of a dust particle is continuously adujusted due to the changing plasma environment towards the local equilibrium value [21]. Saturn's ring system was first observed by Voyager 1 and was found to consist of numerous "ringlets" along with the densest portions of B ring consisting of various nonaxisymmetric features [22]. Nearly radial "spokes" were observed which appeared as dark wedge-shaped rotating radial markings in the outer portion of the Saturn's B ring. The

rotation of the spokes was found to be periodic by Porco and Danielson [23] with a period of 621 ± 22 min. The variations of spoke activity was first thought to be due to the changing illumination of the rings, as the solar elevation angle increased due to the orbital motion of the Saturn. However, Cassini didn't find the spokes on its approach towards Saturn and after its orbital insertion in July 2004 and September 2005 respectively which suggests that the spokes are seasonal phenomena and their formation can be suspended. Goertz and Morfill suggested that the spokes consist of micron sized dust particles elevated from the rings by radially moving plasma column generated from meteor impacts on the ring. According to them, a spoke is a radial dust trail formed by the lifted off dust particles due to the radially moving plasma column [24]. The shape of the spokes was explained on the basis of magnetosonic waves which were shown to give rise to such radial structures in the neighbourhood of the corotation of a thin Keplerian ionized disk [25].

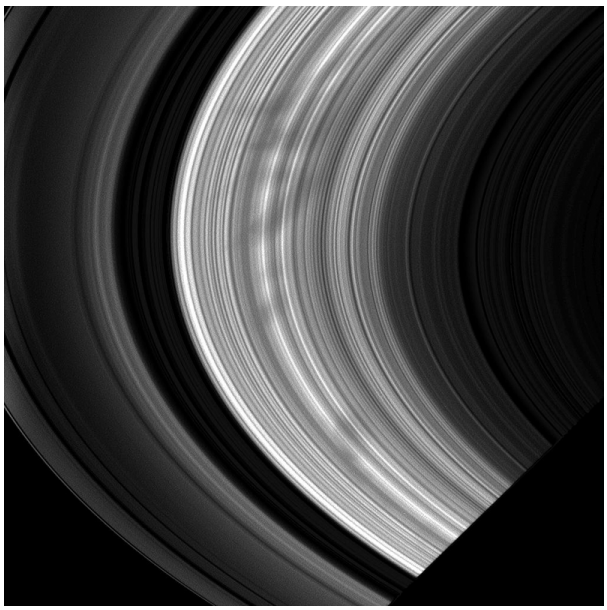

Figure 1.2: Spokes of saturn ring visible as dark radial smudges in the middle of the rings. Photograph distributed under CC BY-SA 2.0 license and taken from Wikimedia Commons.

1.4.2 Dusty plasma in laboratory

The appearance of dust particles in a discharge plasma was first noted by I. Langmuir in 1924 [26]. At that time the dust particles were treated as dirt-effect to the plasma and no specific research effort was directed towards the study of the physics of dusty plasmas [5]. However, during the late 1980s the presence of dust particles in plasma processing of semiconductor chips and microelectronics became a problem for the industries. It was found that particulate contamination has detrimental effects on device topography, performance, reliability and yield [27]. Dusty plasma is studied in laboratories using dc or rf discharges. Most of the noteworthy dusty plasma experiments in the past have been performed in rf discharges [28]. In low pressure conditions of dc or rf discharges the electron transport is non-local in nature [29]. In a dc glow discahrge, striations are formed. Striations are ionization instabilities in the positive column of the dc discharge. The dust particles are trapped in the striations due to high charge on the grains and strong axial and radial gradients of potential in the head of the striations and can form ordered structures [30]. Ordered structures of dust particles under microgravity have been investigaged using dc discharges. Various quantities like temperature, concentration, pair correlation function, self diffusion coefficients were measured for different discharge currents [31]. Capacitively coupled rf discharges were also used in both ground based and microgravity complex plasma researches. Earlier in CCRF discharges one rf electrode and one grounded electrode was used, whereas now-a-days both of the electrodes used are rf electrodes. Moreover, a modified version of the standard rf discharge chamber known as Gaseous Electronic Conference radio-frequency Reference Cell is also widely used now-a-days [32].

To numerically model Capacitively coupled rf discharges a PIC/MCC scheme or fluid models with transport coefficients obtained from kinetic simulations are used [32]. In the PIC/MCC scheme the usual Particle - In - Cell method is combined with a Monte Carlo collison approach to model the collision of the dusts with the neutral particles. The spectral emission/excitation of argon and helium atoms in a rf discharge plasma with and without dust have been studied using both PIC/MCC scheme and experiments by Melzer *et al.* [33]. Killer *et al.* studied the

electron heating in capacitively coupled rf discharge argon plasma in the presence and absence of dust and the electron heating was found to be happening in the entire bulk plasma (Ω mode) in the presence of dust whereas it is due to expanding sheath mode in dust-free case (α mode). Particle-In-Cell simulation was carried out which confirmed the experimental findings [34]. It was found that the excitation in the bulk of the discharge is enhanced in the presence of dust whereas in the sheath it is slightly reduced. Goedheer *et al.* used hydrodynamic 2D cylindrically symmetric models and kinetic 1D PIC/MCC approaches to model capacitively coupled rf discharges and applied to microgravity discharges besides studying dust charging process in decaying plasmas [35].

The PIC/MCC scheme is also used to model dc discharges. For example, to model the dc discharge on the PK-4 facility on board ISS in microgravity conditions PIC/MCC simulation has been used by Hartmann *et al.* [36]. They determined the local plasma parameters from the PIC/ MCC simulation which were subsequently used to perform dust dynamics simulations.

In laboratories, the dust grains charge up due to electron and ion flux onto their surfaces. The grain charge can be such that the floating potential on the grain surface can be equal to electron temperature ($Z_d e^2/a \simeq T_e$) and the charge becomes proportional to the grain size ($Z_d \propto a$) [6]. This makes it possible for the grains of size $\sim 10\,\mu m$ to attain charge as high as $10^4 - 10^5$ times the electronic charge. Because of the large charge on the grains, the grain-grain interaction potential energy can far exceed the kinetic energy of the dust grains. This makes it possible for the dust subsystem to achieve much stronger coupling than the ion subsystem. This was shown by Ikezi in 1986 theoretically. Experimentally, later it was shown that solid and crystalline state can indeed exist in complex plasmas.

In ground based laboratories, it is difficult to achieve homogeneous and isotropic extended three-dimensional complex plasma in the bulk of the discharge because of the effect of gravity on the massive dust particles. Because of gravity, the dust particles settle into the sheath region and remain levitated due to an applied dc electric field [37]. To study phenomena relevant to the extended three-dimensional dust clouds it therefore became necessary to perform those experiments in condi-

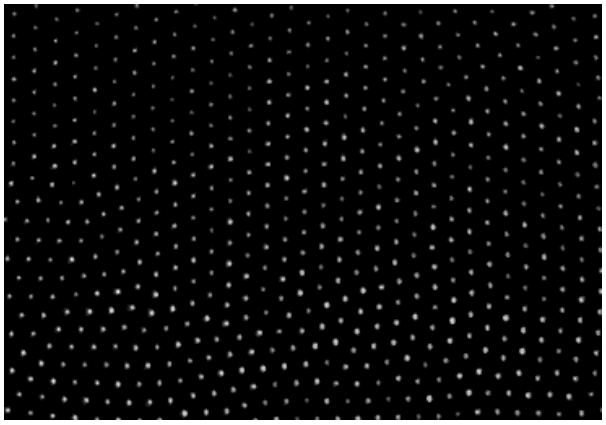

Figure 1.3: Plasma crystal formed by charged dust grains. Photograph distributed under CC BY-SA 2.0 license and taken from Wikimedia Commons. Author : Hubertus Thomas.

tions of low gravity. Therefore, the researchers have devised experimental setups which have been used to perform experiments onboard the International Space Station. Some such experimental facilites include PKE-Nefedov, PK-3 plus and PK-4. Complex plasma research under microgravity includes but is not limited to the study of various condensed - matter phenomena. For example, the theoretically predicted bcc phase was first reported by Nefedov *et al.* in ref. [38] on the PKE-Nefedov facility. The phase behaviour of 3D dusty plasma was investigated by Khrapak *et al.* and they found that by tuning neutral gas pressure phase change can be affected [39]. They attributed the observed phase change to change in electrical repulsion among the particles upon changing the neutral pressure. Propagation of dissipative solitary waves was studied in a binary complex plasma on the PK-3 plus facility by Sun *et al* [40]. The solitary wave was found to propagate from the the sub-system of smaller particles to that of larger particles. They also performed a Langevin Dynamics simulation of the binary complex plasma by taking into account of ion-drag force where a push was given to the sub-system of smaller particles and the wave was allowed to reflect from the interface of the two sub-sytems.

1.5 Forces on a dust grain in complex plasma

A dust grain in complex plasma experiences different forces which govern its dynamics. Some of the forces experienced by a dust grain have been explained below [15]:

- **Electric force :** A dust particle in complex plasma experiences electric force due to the charge present on the grain. The expression of the force can be written as,

$$\mathbf{F}_{el} = q_d \mathbf{E}. \tag{1.11}$$

  The electric field force aids in levitating the dust particles in the sheath region where there exists very strong electric field.

- **Gravity :** The dust particles experience gravitational force due to the gravitational field of the Earth which is simply, $\mathbf{F}_g = m_d \mathbf{g}$. Of course, the mass of a dust grain depends upon the radius of the dust grain as $m_d \propto r_d^3$ which results in a very small gravitational force for smaller dust grains. Only for larger dust grains the gravitational force is significant.

- **Thermophoretic force :** Thermophoretic force arises in a complex plasma due to the temperature gradient in the neutral atoms. This force is exerted from the hotter region towards the colder region of the neutral gas. Mathematically it has been derived by using kinetic theory as follows :

$$\mathbf{F}_{th} = -\frac{32 r_d^2 k_n}{15 v_{th,n}} \nabla T_n, \tag{1.12}$$

  where, k_n is the thermal conductivity of the neutral gas, $v_{th,n}$ is the thermal velocity of the neutral atoms, r_d is the radius of a dust particle and T_n is the temperature of the neutral gas. The thermophoretic force has been used in levitating dust grains in complex plasma as well as creating a harmonic confining potential.

- **Ion-drag force :** A dust grain can be affected by a streaming specie like ions or neutral atoms. A drag force can be expressed in general as follows :

$$\mathbf{F}_{drag} = \Delta p n e \sigma \mathbf{v}_{rel}, \tag{1.13}$$

where, n is the density of the streaming specie, σ is the collision crossection, Δp is the transferred momentum and $\mathbf{v}_{rel}$ is the relative velocity of the streaming specie with respect to a dust grain. Ion streaming can affect a dust particle in two ways : by directly hitting a dust grain or due to Coulomb scattering. The force on the dust grain due to direct ion hitting can be expressed as,

$$\mathbf{F}_{dir} = \pi r_d^2 n_i v_s m_i \mathbf{u}_i \Big(1 - \frac{2e\phi_{fl}}{m_i v_s^2}\Big). \tag{1.14}$$

In the above equation, mean velocity is defined as $v_s = \sqrt{u_i^2 + v_{th}^2}$ where, u_i is the ion streaming velocity, ϕ_{fl} is the dust floating potential, and v_{th} is the ion thermal velocity. The ions while streaming past a dust particle are influenced by the electric field of the dust grain and hence get scattered. The force on the dust particles due to this scattering is given as,

$$\mathbf{F}_{Coul} = 2\pi \frac{r_d^2 e^2 \phi_p^2}{m_i v_s^3} n_i \mathbf{u}_i \ln\Big(\frac{\lambda_D^2 + b_{\pi/2}^2}{b_c^2 + b_{\pi/2}^2}\Big). \tag{1.15}$$

In the above equation, $b_{\pi/2}$ is the impact parameter for 90° deflection. The total ion drag force on a dust particle is,

$$\mathbf{F}_{drag} = \mathbf{F}_{dir} + \mathbf{F}_{Coul}. \tag{1.16}$$

- **Polarization force :** Polarization force on a dust particle arises due to the dipole moment on a dust particle or due to the dipole moment of the shielding cloud. The polarization force on a dipole is :

$$\mathbf{F}_{dip} = \nabla\Big(\mathbf{p}.\mathbf{E}\Big). \tag{1.17}$$

In a dusty plasma, the dipole moment on a dust grain may arise due to directed charging which means that the dust particle gets hit from one side more than from other side by the streaming ions. A dust particle near the sheath experiences large ion flux from from the bulk of the plasma than from the bottom side which makes one side more positive than the other side.

1.6 Collective modes in complex plasmas

Complex plasmas support various low-frequency wave modes as well as instabilities which are not present in a conventional electron-ion plasma besides some other wave modes in modified form that are already present in an electron-ion plasma. Complex plasmas in gaseous form occurs when there is sufficient energy influx in to the system of grains therby increasing the grain temperature. In the gaseous or weakly coupled state the analysis of wave modes becomes much simpler and the effects of strong coupling can be added afterwards. Moreover, the presence of an external magnetic field may introduce new wave modes in to the complex plasma. The wave modes in plasmas can be studied from two different perspectives: using a fluid description or using a kinetic approach. The fluid description is physically more transparent as the physical observabables like pressure, number densities and fluid velocities can be easily obtained [41]. In the kinetic description one normally starts with the Klimontovich or Liouville equation of some phase space density of the system. The reduced phase space distribution functions of the system are used instead of the full phase space distribution functions which obey the BBGKY hierarchy of the equations [41]. The waves in complex plasma can be broadly classified into two categories: the wave modes arising in a strongly coupled complex plasma and those arising in weakly coupled complex plasma. The waves in strongly coupled complex plasma are known as Dust Lattice Waves (DLW) and the waves in weakly coupled dusty plasma are mainly Dust Acoustic Waves (DAW) or Dust Ion Acoustic Waves (DIAW) [15]. Brief descriptions of some of the wave modes are given below :

- **Dust Acoustic Waves :** In dust-acoustic waves the dust particles are mobile species and electrons and ions in the background remain in thermodynamical equilibrium [42]. These are low frequency waves because of the high dust mass. The frequencies of the DAWs are of the order of dust-plasma frequency $\omega_{pd} = \sqrt{\frac{q_d^2 n_d}{\epsilon_0 m_d}}$, where, n_d is the equilibrium dust density, q_d is the dust charge and m_d is the dust mass. The dispersion relation for the DAWs is [4]:

$$\omega^2 = 3k^2 V_{Td}^2 + \frac{k^2 C_D^2}{1 + k^2 \lambda_D^2} \tag{1.18}$$

In the limit $\omega >> kV_{Td}$ and in the long wavelength limit $k^2\lambda_D^2 << 1$,

$$C_D = \omega_{pd}\lambda_D. \tag{1.19}$$

DAW was first theoretically predicted by Rao *et al.* [42]. Laboratory observation of Dust Acoustic Waves was first reported by Barkan *et al.* [43] and then subsequently by other researchers. Pieper and Goree [44] investigated the low frequency compressional waves in a strongly coupled dusty plasma. They found that the dispersion relation for a damped weakly coupled dusty plasma also explains the dispersion of a strongly coupled dusty plasma but not the dispersion relation of strongly coupled lattice wave model. The dispersion relation of Dust Acoustic Waves (DAW) in dc glow discharge plasma was measured by Thompson *et al.* [45]. Merlino *et al.* [46] studied the dust acoustic wave where the dust particles were levitated by applying an electric field and the experimentally measured dispersion relation matched with theoretical prediction with the dust-neutral collision taken into account. Fortov *et al.* also studied spontaneously excited low frequency waves in a dc glow discharge dusty plasma in the presence of dust-neutral collisions, dust charge variations, ion drift, and forces acting on the dust particles and found that the instability was observed due to dust charge variations in the presence of charge dependent forces on the dust particles and ion-drift effect [47].

- **Dust Ion-Acoustic Wave :** In DIA waves, the ions take part in the wave dynamics whereas the dusts remain stationary and the electrons remain in the background in thermodynamical equilibrium. Although the dust particles don't take part in the wave dynamics, they indeed affect the electron density by reducing it as the elecrons attach to the dust surface. The dispersion relation for DIA waves can be written as,

$$\omega^2 = \frac{\omega_{pi}^2\lambda_{De}^2k^2}{1 + k^2\lambda_{De}^2}. \tag{1.20}$$

In the long wavelength limit $(k \to 0)$ this yeilds the sound speed:

$$\frac{\omega}{k} = \sqrt{\frac{n_{i0}k_BT_e}{n_{e0}m_i}}. \tag{1.21}$$

It can be seen that the sound speed of DIAW is larger than that of Ion-Acoustic Waves as $n_{i0} > n_{e0}$ in a dusty plasma with negatively charged dust

grains [48]. Experimentally, Barkan *et al.* observed the increase in phase velocity of Ion Acoustic waves due to the presence of dust particles in plasmas besides a decrease in collisionless damping (Landau damping) [43]. Merlino *et al.* also examined the effect of dusts in ion-acoustic and electron-ion cyclotron waves in plasmas and found that the presence of charged dust particles modifies these wave modes via the modification of the quasineutrality condition [46].

- **Dust lattice waves :** In the strongly coupled state Dust Lattice Waves (DLW) are excited in a dusty plasma. As it is clear from the name itself, for this type of wave to be excited in a dusty plasma a crystalline dusty plasma is required. DLW can be excited in a 1D chain of dust particles, in a 2D dust crystal as well as in a 3D dust crystal. In 2D, the DLW can propagate as compressional (longitudinal) wave, shear wave or transverse wave. The dispersion relation of compressional waves in a linear chain of dust particles can be expressed as,

$$\omega(k) = 2\sqrt{\frac{K}{m}}\sin\Big(\frac{kr_{av}}{2}\Big), \tag{1.22}$$

where, K is the spring constant. In a 2D monolayer of dust particles in strongly coupled complex plasma, the longitudinal and transverse dispersion relations are as follows,

$$\omega_l(\omega_l + i\nu) = 2\sum_{X,Y,Z} F(X,Y,Z)\sin^2\Big(\frac{kX}{2}\Big) \tag{1.23}$$

$$\omega_t(\omega_t + i\nu) = 2\sum_{X,Y,Z} F(Y,X,Z)\sin^2\Big(\frac{kX}{2}\Big). \tag{1.24}$$

In the above, $F(X,Y,Z)$ is defined as,

$$F(X,Y,Z) = R^{-5}e^{-\kappa R}[X^2(3+3\kappa R+\kappa^2R^2) - R^2(1+\kappa R)], \tag{1.25}$$

and it is the normalized spring constant where, $R = \sqrt{X^2+Y^2+Z^2}$ is the equilibrium position of a dust particle in dimensionless units [49].

- **Cyclotron modes :** Additional wave modes are observed in a complex plasma in the presence of an external magnetic field. As in an electron-ion plasma the presence of an external magnetic field significantly modifies

the dispersion properties of the waves in a dusty plasma. These waves propagate nearly perpendicularly to the externally applied magnetic field. The Electrostatic Dust Ion-Cyclotron (EDIC) mode is a modification of the Electrostatic Ion Cyclotron (EIC) Wave due to the presence charged dust. Considering, the dust to be immobile species i.e; $\omega \sim \Omega_{ci}$, the dispersion relation becomes [46],

$$\omega^2 = \Omega_{ci}^2 + K_x^2\Big[\frac{k_B T_i}{m_i} + \frac{k_B T_e}{m_i\Big(1 - \frac{n_{d0}Z_d}{n_{i0}}\Big)}\Big]. \tag{1.26}$$

In the above equation, Ω_{ci} is the ion cyclotron frequency, K_x is the wavevector along $x-$direction, m_i is the ion mass, n_{d0} and n_{i0} are respectively the equilibrium dust and ion densities, T_e and T_i are respectively the electron and ion temperatures and Z_d is the dust charge number respectively. Similarly, the Electrostatic Dust Cyclotron (EDC) mode is obtained if the dust dynamics is taken into consideration. The dispersion relation for EDC mode is,

$$\omega^2 = \Omega_{cd}^2 + K_x^2\left[\frac{k_B T_d}{m_d} + \frac{n_{d0}Z_d^2 k_B T_i}{m_d n_{e0}\Big(1 + T_i/T_e(1 - \frac{n_{d0}Z_d}{n_{e0}})\Big)}\right]. \tag{1.27}$$

In the above equation, Ω_{cd} is the dust cyclotron frequency.

1.7 Strongly coupled dusty plasmas

A plasma specie is said to be strongly coupled if the ratio of average interparticle potential energy to the average thermal energy becomes greater than unity for it. That is, the quantity

$$\Gamma = \frac{\Big\langle |V| \Big\rangle}{\Big\langle K \Big\rangle}, \tag{1.28}$$

is greater than unity for any strongly coupled plasma specie. This means that for strong correlaton to occur the plasma density has to be sufficiently large and the kinetic temperature has to be sufficiently smaller. If an electron-ion plasma is sufficiently compressed so that the thermal De Broglie wavelength ($\lambda_e = \frac{\hbar}{\sqrt{2mk_BT}}$) becomes comparable to the ion-electron interaction radius (Ze^2/k_BT) then quantum description is needed for such kind of plasma [50].

Strong correlation among particles affects the spatial arrangement of the particles in a plasma besides affecting the distribution of the particles in momentum space [51]. The effects of strong correlation in spatial distribution of particles is reflected in the static structural quantities like Radial Distribution Function, static structure factor etc.

Most of the classical plasmas remain however in a weakly coupled state i.e, $\Gamma << 1$ for such systems. In a weakly coupled state the behaviour of the system of particles resembles that of an ideal gas. In nature, strongly coupled classical plasmas occurs in high density environments such as the system of ions inside a white dwarf star in the background of degenerate electron plasma, the ion plasma in the interior of a jovian planet etc [52].

Dusty plasma is a kind of plasma which consist of electrons, ions, neutral gas and highly charged particles of size ranging from nano to micrometer. The values of charge on the dust grains can reach upto the order of $10^3 - 10^4 e$ where, e denotes electronic charge. Due to the high charge on the dust grains the nonideality for the dust subsystem can be achieved at relatively low dust density and high temperature than the electron or ion subsystems which makes it possible to observe many different states in dusty plasma: fully disordered gaseous state ($\Gamma << 1$), liquid like state having short ranged order ($\Gamma > 1$) and solid like long range order ($\Gamma >> 1$) [50]. As already given in section 1.2.4 a dusty plasma enters into a crystalline regime once $\Gamma_{eff} = \Gamma \exp(-\kappa) > 168$. Strongly coupled dusty plasma have been used as a model system to study various phenomena relevant to condensed matter. Because of the large size and mass on the grains the phenomena can be observed at individual kinetic level in dusty plasma experiments. This therefore resembles an atomistic treatment of a classical condensed matter system. Due to the presence of neutral damping the dust grains loss energy therby lowering its kinetic temperature and the dust subsystem therefore can attain a strongly coupled state.

The thermodynamic properties of a strongly coupled Yukawa system was studied by Hamaguchi *et al.* both using analytical therories and Molecular Dynamics simulations [53, 54, 55, 56]. Hamaguchi and Farouki derived the expressions of excess

energy for a strongly coupled Yukawa system under periodic boundary conditions in the limit of weak screening which can be used in Monte Carlo or Molecular Dynamics simulations to obtain thermodynamic properties [53]. They found that the pair potentials that may be derived from the total potential energy admits an attractive part superimposed over a repulsive Yukawa potential which is actually incorrect. The attractive potential arises from the consideration that the Debye sheath around a test particulate is attached to the it and forms therby a single system. However, the space charge around a test particulate is a perturbation to the background plasma due to the charge on the particulate. Therefore, the Debye sheath are actually not attached to the particulate at all and can form in a place within the plasma to where the particulate relocates. The ideal part of the Helmholtz free energy of the backgrond plasma exactly cancels the attractive potential of the internal energy therby making the interparticle interaction just Yukawa potential. Molecular Dynamics simulations were also performed to obtain the free energies in the solid and liquid phases of the Yukawa system in the weak screening limit as an extrapolation of the One Component Plasma (OCP) ($\kappa = 0$) [54]. The location of the phase transition point was found to increase to $\Gamma = 378$ at $\kappa = 1$ from $\Gamma = 171$ at $\kappa = 0$. Later in their work in ref. [56] they found the phase transition points to be occuring at systematically lower values of inverse temperarature than their earlier study in ref. [54] which they attributed to the more accurate calculation of the harmonic entropy constants based upon lattice dynamics instead of approximating the harmonic entropy constants by that of One Component Plasmas. Hamaguchi *et al.* extended their earlier studies to the regime of strong screening where they obtaind the phase diagram exhibiting both fluid-solid and solid-solid phase transitions. The triple point which is the intersection of fluid-solid and solid-solid phase transition curves was found to occur at $\kappa = 4.28$ and $\Gamma = 5.6 \times 10^3$ [55].

1.8 Self-organization in complex plasmas

Self organization refers to a process by which many or a few components of a system form ordered structures spontaneously without being controlled by any external agency. Because there exists a continuous flux of electrons and ions to the

dust surface where they recombine, dust grains in a dusty plasma, act as sinks. To compensate for the loss of plasma particles (electrons and ions) and energy an external ionization source is required. Consequently, a dusty plasma behaves as a thermodynamically open system. The presence of dissipation and thermodynamic openness makes dusty plasma conducive of exhibiting self-organization phenomena [6].

There are various examples of self organization in complex plasmas. For example, the formation of Coulomb crystals by the dust grains in a low-temperature plasma is one of them [57, 58]. Although plasma is considered one of the most disordered state of matter, the micron sized dust particles when introduced into the plasma can spontaneously form ordered crystalline pattern of particles [59]. In the presence of ion-flow dust particles were shown to attract each other due to collective interactions involving ion-oscillations in the flow. It was also shown that a lattice can form in such a scenario in the electrostatic sheath of dust plasma boundary [60]. The dust particles exhibit vertical alignment in complex plasma which is seen in the presence of ion-flow. Schweigert *et al.* showed that the formation of positive space charge region below a dust particle gives rise to an attractive interaction between two dust grains leading to the formation of such vertically alinged dust layers [61]. Self-organized one-dimensional vertical chains, two-dimensional zig-zag structures, and three-dimensional helical structures with triangular, quadrangular, pentagonal, hexagonal and heptagonal symmetries were studied by Hyde et. al. [62]. The transition between one-dimensional to two-dimensional structures and two-dimensional to three-dimensional structures were affected by changing the anisotropy parameter and defined as $\gamma^2 = \left(\omega_{0h}/\omega_{0v}\right)^2$, $\omega_{0h,v}$ being the dust resonance frequencies. The anisotropy parameter was shown to be a function of both rf power and total number of particles.

Another example of self-organized structure is the formation of dust free regions or the so-called "voids". Praburam and Goree observed the formation of voids in a dusty plasma experiment where they detected a rotating region without any detectable dust. This low frequency mode was termed as the great dust void mode in their work [63]. Subsequently, theoretical explanation of the formation of dust voids in plasmas was given by Goree et. al. [64]. Dust voids were shown to arise

due to the balance between electrostatic and ion drag forces on a dust particle. They also found that to sustain a void there has to be a sufficient ionization rate. There has been a number of other experimental observations and theoretical studies of dust voids in complex plasmas so far [65, 66, 67]. Recently, the disagreement between the observed microparticle arrangement and spatiotemporal emission spectrum revealed a lack of accurate description of sharp void boundary in fluid approach [68].

Besides these, the formation of vortices were also seen in complex plasmas. Vortex movement of dust particles were observed in nuclear induced plasmas in atmospheric air with micron sized charged dust particles [69]. The dusty plasma was formed by electron beta-decay from the dust particles and passage of alpha particles and fission fragments of Californium-252 nuclei through dust grains. They observed that when an electric field existed in the interelectrode space, vortex movements of dust particles occurs in the plane of the laser sheet. Vortex formation also was observed in microgravity complex plasmas. Morfill *et al.* observed stable three dimensional vortex flows in microgravity complex plasmas [70]. They observed that with reduction in rf power the ordered vortex flow breaks up into several smaller vortices of the size of 10 to 18 particle spacings. Stable vortex flows are possible in a dissipative dusty plasma in the presence of external sources of energy [71]. Viscoelastic vortical fluid motion was observed by Ratynskaia *et al.* in a two dimensional complex plasma. The motion of the particles were found to be superdiffusive and the superdiffusion mechanism was found to obey Levy statistics on short time scales and memory effets on longer time scales affected by cooperative motion [72]. Vaulina *et al.* studied the instability of a plasma-dust system in the presence of spatially varying macroparticle charge of a dust cloud in a trap formed by an external electric field and gravitational field. The mathematical models for the non-linear non-equilibrium system admits two types of instabilities: type I and type II. The equations for type I instability may describe vortex convective motion [71].

Another example of self-organization in complex plasmas is the formation of Lanes. Lane formation takes place when some particles of smaller size are driven against the particles of larger size and the like-driven particles form streams [73]. The

dynamics of laning in binary complex plasma was investigated in microgravity conditions by Sutterlin *et al.* [73] by combined studies of experiment and Langevin Dynamics simulations. The inflowing smaller particles penetrated the bigger particle system pushing the bigger particles collectively thereby creating strings and the smaller strings then organize themselves to give rise to larger streams of particles. They also obtained an anisotropic scaling index which led to a universal order parameter for driven systems. It was shown that the dynamics of lane formation varies considerably depending on the density of the background particles and the size ratio of the bigger and smaller particles. There also occurs a crossover from lane formation to phase separation where the smaller particles cage the bigger background particles [74]. The process of lane formation as shown by Du *et al.* proceeds via three stages. First the smaller particles are pushed to the background of bigger particles by the inhomogeneous plasma potential. Then lane formation occurs. Finally, the smaller particles move towards the center where the driving force on the smaller particles decreases and phase separation of the smaller and bigger particles starts and the smaller particles form a droplet. During this process some bigger particles remain inside droplet formed by the smaller particles and form lanes [74, 75].

1.9 Finite clusters in dusty plasmas

Finite systems, that is systems consisting of a small number of particles appear in different physical systems. Historically, the Thomson problem marked the beginning of research on finite strongly coupled systmes [51]. Some such systems include electrons at the surface of liquid helium, electrons in quantum dots, ions in Paul or Penning trap etc. Transition from a homogeneous charge distribution to an ordered pattern is shown by electrons trapped near the surface of liquid He with change in perpendicular electric field [76]. Quantum dot is another example of finite trapped system where a very small number of electrons can be confined in a box having side length about 100 nm. It has been possible to perform atomic physics experiments with the help of quantum dots in a regime which is not accessible in experiments on real atoms [77]. Ions or electrons can be trapped by using confining potential in Paul or Penning traps for several hours or days

in thermal equilibrium [78].

In dusty plasma also finite clusters appear as chain of particles, monolayer of particles and as three-dimensional structures [15]. Static, dynamic and thermodynamic properties of these finite clusters show significant deviation from that of bulk homogeneous systems. Such a system of N particles interacting via pairwise additive Yukawa potential and confined by a global harmonic oscillator potential can be modeled by the following Hamiltonian:

$$H = \sum_{i=1}^{N} \frac{\mathbf{p}_i^2}{2m} + \frac{q_d^2}{4\pi\epsilon_0} \sum_{i=1}^{N-1} \sum_{j=i+1}^{N} \frac{\exp(-r_{ij}/\lambda_d)}{r_{ij}} + \frac{1}{2} m\omega_0^2 \sum_{i=1}^{N} \mathbf{r}_i^2, \tag{1.29}$$

where, q_d, m, ω_0 and λ_d denote respectively the charge, mass, confining strength and d Debye length corresponding to dust particles and r_{ij} is the interparticle distance between ith and jth partilces. It is observed that the particles in a harmoniclally trapped finite three-dimensional dust cluster arrange themselves in nested spherical shells and in a two-dimensional cluster the particles arrange in concentric circles. Unlike bulk systems the finite clusters are actually inhomogeneous. The presence of a confining potential breaks the translational invariance of the system. Although in bulk homogeneous systems the pair correlation function is a suitable quantity to understand the static structure of the system, in finite clusters the violation of translational invariance limits the usefulness of pair-correlation function. So, spatial two- and three- particle correlation functions have been constructed which depend on the exact position of particles in space and sucessfully used in studying structural transitions of finite three-dimensional clusters [79, 80]. A 1D dust cluster can be formed in a laboratory dusty plasma experiment by making a groove in the lower electrode in order to provide the necessary harmonic confinement potential along the x- and y- direction [81]. Gravity is balanced by the electric field force. 1D chain of particles in dusty plasma have been shown to exhibit zigzag transition on varying particle number and confinement strength [82, 83]. 2D clusters can be formed by making a circular trough on the electrode which provides the isotropic parabolic potential necessary for confining the dust particles. In such a 2D cluster the particles arrange themselves into concentric shells. The occupation number of shells obey magic numbers which is akin to the magic numbered nuclei and atoms that shows high stability [15]. The ground state configurations of these clusters have been obtained by adopting an

energy minimization procedure. A “periodic table” was constructed from these ground state configurations [84]. Three dimensional clusters can also be formed in laboratory environments and in this case the harmonic confinement potential is generated due to the superposition of gravitational, thermophoretic, ion drag and electric field force [85]. The particles arrange themselves into nested spherical shells and exhibits high stability corresponding to magic numbered configurations [86]. These three-dimensional clusters are commonly known as ”Yukawa balls” [87].

Dynamic properties of finite dust clusters have also been studied by various workers in some detail. Dynamic properties have been studied in terms of normal modes of the clusters. This is done by first constructing the dynamical matrix and then finding the eigenvalues and eigenvectors which respectively corresponds to the mode frequencies and mode oscillation patterns. A 2D cluster can have several normal modes such as sloshing mode where the entire cluster shows oscillation in the horizontal plane, rotation of the entire cluster, breathing mode where the particles show purely radial oscillations and intershell rotational mode etc [88, 89]. Dynamics of melting process of 2D Yukawa clusters were investigated by using normal mode analysis [90, 91]. The dynamic entropy of finite 2D Yukawa cluster was obtained experimentally as a function of normalized radius of a circle around the particles as the cluster transitions from a metastable state with lower hexagonal symmetry to ground state with higher hexagonal symmetry [92].

1.10 Magnetic field effects in complex plasma

Magnetic fields are ubiquitous in nature. In plasma naturally there exist mangetic fields due to the motion of charged particles. In laboratory experiments one can apply an external magnetic field. The ease with which a plasma specie gets magnetized depends upon the charge-to-mass ratio of that specie. Therefore, with increase in the strength of externally applied magnetic field the electrons first get magnetized and then the ions and if the magnetic field is still increased finally the micron sized dust grains get affected. The low charge to mass ratio of the dust

grains enables the experimentalist to study dust dynamics at the kinetic level. Because of the effect of magnetic field on the dynamics of electrons and ions, the forces on the dust grains which are mediated by the plasma and the dust-dust interaction potential are also modified.

A magnetized dusty plasma can be characterized by various parameters such as the ratio of the Larmour radius (ρ_d) and system size (L) defined as $R_g = \frac{\rho_d}{L}$, the ratio of dust cyclotron frequency (Ω_c) to dust-neutral collision rate (ν_{dn}) defined as $R_c = \frac{\Omega_c}{\nu_{dn}}$ and known as the Hall parameter. For dust particles to be considered magnetized, the ratio R_g has to be much less than 1 and the ratio R_c should be greater than 1 [93]. Physically, $R_c > 1$ means that a particle completes a full gyro motion before experiencing a collsion with neutrals. There is another parameter called magnetization parmameter (M) defined as the ratio of dust cyclotron frequency (ω_{cd}) to dust plasma frequency (ω_{pd}) i.e, $M = \frac{\omega_{cd}}{\omega_{pd}}$, which should be greater than 1 for dust particles to be magnetized. When this parameter is greater than unity it means that the motion of a dust grain mainly is governed by the magnetic field than by electrostatic interactions. The equivalence of magnetic Lorentz force and Coriolis force in a rotating frame of reference has been exploited to study high magnetic field effects on complex plasma. In these experiments, the angular momentum of a rotating neutral gas column is transferred to the dust subsystem [94]. This makes the dust grains behave as if they are magnetized whereas, the electrons and ions remain unmagnetized.

Various intriguing phenomena are observed in dusty plasmas under the effect of strong external magnetic field. Filamentation, rotation of dust cluster and formation of imposed structures etc are some of the examples [95]. Filamentary structures are the regions in plasma which are aligned along the magnetic field lines and have high optical brightness[96]. These structures can form in plasmas with dusts or without dusts [97]. The filamentation transition occurs at lower gas pressures. It has also been observed that in magnetized dusty plasmas the structure of walls or electrodes are mapped onto the plasma due to the directionality induced by the magnetic field [98]. Rotation of dust structures is one of the most studied phenomenon in magnetized dusty plasmas [99, 100, 101, 102, 103, 104]. This rotation arises because of the fact that a sufficiently strong external mag-

netic field induces rotation on to the ions and the ions transfer that rotation to the dust structure via ion-drag force. This model of rotation agrees well with experiments at lower values of neutral pressure but at higher values this yeilds too low a rotation speed. At higher neutral pressure, the model is therefore modified to include the rotation of neutral gas due to ion-neutral collision which in turn rotates the dust structure.

1.11 Magnetized dust cluster

Various phenomena like rotation, normal modes and phase transition of finite harmonically confined dust clusters have been studied in the presence of magnetic field in experiment, theory and simulation. Slow rotation of strongly coupled quasi-2D dust cluster under moderate magnetic field was observed by Juan *et al.* [105]. Ishihara *et al.* did a combined theoretical, experimental and simulational analysis where the charged dust particles were shown to form a ring shaped cluster in the horizontal plane with a radius determined by the balance between confining harmonic and repulsive Yukawa force. In the presence of a perpendicular magnetic field the cluster shows rotation about the magnetic field direction and the angular frequency of rotation as a function of cyclotron frequency has been theoretically calculated and compared with simulation [104]. The effect of neutral gas motion on the rotation of dust clusters in the presence of a perpendicular magnetic field has been investigated experimentally [101]. This shows that unlike some interpretation of rotation of dust clusters due to ion-drag force the rotation is actually driven by the neutral gas which rotates due to ion-neutral collision and advects the dust particles by this flow.

1.12 Methodology

1.12.1 Numerical simulation of finite dust clusters

To numerically simulate finite dust clusters in plasma environment frictionless Molecular Dynamics (fMD) and Langevin Dynamics (LD) simulation method has been used in this thesis. In fMD simulation, equations of motion of the particles

are integrated to obtain the positions and velocities of the particles at each time step:

$$m\ddot{\mathbf{r}}_i = -q_d \sum_{j\neq i}^{N} \nabla\phi(r_{ij}) + \mathbf{F}_{ext}. \tag{1.30}$$

In the above equation, $\mathbf{r}_i$ is the position of the i^{th} particle, ϕ is the interparticle potential operative among the dust grains and $\mathbf{F}_{ext}$ is the external force on the i^{th} dust particle. Molecular Dynamics simulation is performed on the particles distributed inside a simulation box. We use velocity verlet algorithm to integrate the equations of motion. Molecular Dynamics predicts the time evolution of particle trajectories in phase space. In our simulation,

$$\phi(r_{ij}) = \frac{q_d}{4\pi\epsilon_0 r_{ij}} \exp(-\kappa r_{ij}), \tag{1.31}$$

and,

$$\mathbf{F}_{ext} = -m\omega^2 \mathbf{r}_i. \tag{1.32}$$

In the above equations, q_d is charge on the dust grains which is assumed to be constant, κ is screening parameter which is inverse of Debye length of the dust grains and $r_{ij} = |\mathbf{r}_i - \mathbf{r}_j|$ is interparticle distance, ω is strength of the external potential, m is mass of the dust particles and $\mathbf{r}_i$ is distance of any particle from the center of the simulation box. Initially, the particles are randomly distributed in a cubical simulation box of length L. The random initial velocities are chosen according to the target temperature and initial accelerations are determined from the initial positions of the particles that can be calculated from the potential energy function.

To integrate the equations of motion, we make use of the velocity-verlet algorithm which is obtained through Taylor expansion of positions and velocities [106],

$$\mathbf{r}(t+\delta t) = \mathbf{r}(t) + \delta t\mathbf{v}(t) + \frac{\delta t^2}{2}a(t) \tag{1.33}$$

$$\mathbf{v}(t+\frac{\delta t}{2}) = \mathbf{v}(t) + \frac{\delta t}{2}\mathbf{a}(t) \tag{1.34}$$

$$\mathbf{a}(t+\delta t) = \mathbf{a}(\mathbf{r}_1(t+\delta t), \mathbf{r}_2(t+\delta t).....\mathbf{r}_N(t+\delta t)) \tag{1.35}$$

$$\mathbf{v}(t+\delta t) = \mathbf{v}(t+\frac{\delta t}{2}) + \frac{\delta t}{2}\mathbf{a}(t+\delta t) \tag{1.36}$$

In a typical simulation run, the number of particles, volume and temperature are kept fixed. The system is brought to equilibrium by rescaling the velocities at

each timestep for a certain number of time steps and data is collected during the next couple of steps to measure various properties.

In presence of magnetic field, the equation of motion of the i^{th} particle becomes :

$$m\ddot{\mathbf{r}}_i = -q_d \sum_{j \neq i}^{N} \nabla\phi(r_{ij}) + q_d(\mathbf{v_i} \times \mathbf{B}) + \mathbf{F}_{ext} \tag{1.37}$$

The magnetic field in our MD simulation has been implemented via a modified version of velocity-verlet algorithm[107]. With the help of this algorithm it is possible to take arbitrarily large magnetic field in MD simulation. The algorithm is as follows :

$$\begin{aligned} r_x(t+\Delta t) =& r_x(t) + \frac{1}{\Omega}\Big[v_x(t)\sin(\Omega\Delta t) - v_y(t)C(\Omega\Delta t)\Big] \\ &+ \frac{1}{\Omega^2}\Big[-a_x^C(t)C(\Omega\Delta t) - a_y^C(t)S(\Omega\Delta t)\Big] \\ &+ O((\Delta t)^3) \end{aligned} \tag{1.38}$$

$$\begin{aligned} r_y(t+\Delta t) =& r_y(t) - \frac{1}{\Omega}\Big[-v_y(t)\sin(\Omega\Delta t) - v_x(t)C(\Omega\Delta t)\Big] \\ &+ \frac{1}{\Omega^2}\Big[-a_y^C(t)C(\Omega\Delta t) + a_x^C(t)S(\Omega\Delta t)\Big] \\ &+ O((\Delta t)^3) \end{aligned} \tag{1.39}$$

$$r_z(t+\Delta t) = r_z(t) + \Delta t v_z(t) + \frac{1}{2}(\Delta t)^2 a_z^C(t) + O((\Delta t)^3) \tag{1.40}$$

Similarly, the velocities are propagated as follows :

$$\begin{aligned} v_x(t+\Delta t) =& v_x(t)\cos(\Omega\Delta t) + v_y(t)\sin(\Omega\Delta t) + \frac{1}{\Omega}\Big[-a_y^C(t)C(\Omega\Delta t) + a_x^C(t)\sin(\Omega\Delta t)\Big] \\ &+ \frac{1}{\Omega^2}\Big[-\frac{a_x^C(t+\Delta t) - a_x^C(t)}{\Delta t}C(\Omega\Delta t) - \frac{a_y^C(t+\Delta t) - a_y^C(t)}{\Delta t}S(\Omega\Delta t)\Big] \\ &+ O((\Delta t)^3) \end{aligned} \tag{1.41}$$

$$\begin{aligned} v_y(t+\Delta t) =& v_y(t)\cos(\Omega\Delta t) - v_x(t)\sin(\Omega\Delta t) - \frac{1}{\Omega}\Big[-a_x^C(t)C(\Omega\Delta t) - a_y^C(t)\sin(\Omega\Delta t)\Big] \\ &+ \frac{1}{\Omega^2}\Big[-\frac{a_y^C(t+\Delta t) - a_y^C(t)}{\Delta t}C(\Omega\Delta t) + \frac{a_x^C(t+\Delta t) - a_x^C(t)}{\Delta t}S(\Omega\Delta t)\Big] \\ &+ O((\Delta t)^3) \end{aligned} \tag{1.42}$$

$$v_z(t+\Delta t) = v_z(t) + \frac{1}{2}\Delta t\Big[a_z^C(t) + a_z^C(t+\Delta t)\Big] + O((\Delta t)^3) \tag{1.43}$$

Here,

$$S(\Omega\Delta t) = \sin(\Omega\Delta t) - \Omega\Delta t \tag{1.44}$$

$$C(\Omega\Delta t) = \cos(\Omega\Delta t) - 1 \tag{1.45}$$

$$\Omega = \frac{q_d B}{m} \tag{1.46}$$

$$\tag{1.47}$$

$a^C_{x,y,z}(t)$ is the acceleration computed in the force loop at any time t along any direction x, y or z. This is the part of acceleration which does not depend on velocities or which does not involve the contribution from the Lorentz force experienced by the particles due to the presence of the magnetic field. It is only the accleration experienced by the particles due to the Yukawa potential as well as the confining potential. The effects of the magnetic field enters via Ω which is the Larmour frequency. Δ t is the timestep of MD simulation, B is the magnetic field used in the simulation, m is the mass of a dust particle and q_d is the charge on a dust particle.

In dusty plasma dust grains suffer collisions due to background neutral particles. To take this effect into account, Langevin equation is used. The Langevin equation for a dust grain can be written as :

$$m\ddot{\mathbf{r}}_i = -q_d \sum_{j\neq i}^{N} \nabla\phi(r_{ij}) + \mathbf{F}_{ext} - \nu m\dot{\mathbf{r}}_i + \mathbf{A}_i, \tag{1.48}$$

where, ν is the dust-neutral collision frequency and $\mathbf{A}_i$ is the random force on the i^{th} dust particle with zero mean satisfying the following condition according to the fluctuation dissipation theorem,

$$\left\langle A_{ij}(0)A_{ik}(t)\right\rangle = 2m\nu k_B T_d \delta(t)\delta_{jk}, \quad j,k \in \{x,y,z\}. \tag{1.49}$$

In the above equation, T_d denotes dust kinetic temperature and $\delta(t)$ is the delta function.

1.12.2 Static and dynamic diagnostic quantities :

Various static and dynamic properties of the system can be obtained from the simulation data. Some functions used for this purpose have been described below:

- **Radial Distribution Function (RDF) :** Radial distribution function gives the spatial distribution of particles around a central particle. A radial distribution function can be defined as :

$$g(r) = \frac{1}{n_d N}\Big\langle \sum_{i}^{N}\sum_{j\neq i}^{N}\delta(r - r_{ij})\Big\rangle. \tag{1.50}$$

  Here N is the number of particles. RDF is measurable in radiation scattering experiments. RDF gives the structure of a liquid. For systems having pairwise additive potential among the particles the thermodynamic properties of the system can be expressed in terms of integral of $g(r)$ [108].

- **Center-two-particle correlation function :** Although radial distribution function provides information about the structure of the system, this function by its definition (Eq. 1.50) is suited for a homogeneous and isotropic system of particles only. This function cannot distinguish between intra-shell and inter-shell order in a 3D spherical cluster. So some quantities have been developed by Thomsen *et al.* [79] to study the structural transitions in Coulomb or Yukawa clusters. One of them is the center-two-particle correlation function (C2P). This is a function of two radial coordinates measured from the center of the cluster and one angle between the two radial coordinates. It is defined as the ratio of correlated two particle density to uncorrelated two particle density,

$$f(r_1, r_2, \phi) = \frac{\rho_2^{corr}(r_1, r_2, \phi)}{\rho_2^{uncorr}(r_1, r_2, \phi)}. \tag{1.51}$$

  If one of the radial coordinates is integrated over the range of a shell, the resulting function becomes :

$$f^{int}(r, \phi) = \frac{\rho_2^{corr}(r, \phi)}{\rho_2^{uncorr}(r, \phi)}. \tag{1.52}$$

- **Angular correlation function :** The angular correlation function is obtained by integrating both the correlated and uncorrelated pair densities in the C2P function with respect to the two radial coordinates. So, this can be defined as :

$$f^{ang}(\phi) = \frac{\rho_2^{corr}(\phi)}{\rho_2^{uncorr}(\phi)}. \tag{1.53}$$

While obtaining this function by integrating with respect to the two radial coordinates, the integrations can be performed over the range of a single or two different shells. If r_1 and r_2 are integrated over the range of the same shell $f^{ang}(\phi)$ gives intra-shell angular correlations whereas if r_1 and r_2 are integrated over the range of two different shells $f^{ang}(\phi)$ gives inter-shell angular correlations [79].

- **Variance of block averaged interparticle distance fluctuation :** In macroscopic system different quatities can be defined and obtained from the knowledge of particle positions which exhibit sudden change during melting transition. Some examples are Lindmann parameter which is defined as particle position fluctuation normalized by mean interparticle distance, relative Interparticle Distance Fluctuations (IDF) etc. The IDF is defined as,

$$u_{rel} = \frac{2}{N(N-1)} \sum_{i=1}^{N-1} \sum_{j=i+1}^{N} \sqrt{\frac{< r_{ij}^2 > - < r_{ij} >^2}{< r_{ij} >^2}}. \tag{1.54}$$

In finite clusters, however, these quantities don't exhibit sudden jump during melting. To identify the onset of structural transition in finite clusters we use the stragegy developed in ref. [109]. They have used a quantity called variance of block averaged interparticle distance fluctuations (VIDF) which is obtained by first dividing the simulation duration into blocks of equal length and then calculating urel on each block. VIDF is then defined as:

$$\sigma = \left\langle u_{rel}^2 \right\rangle - \left\langle u_{rel} \right\rangle^2. \tag{1.55}$$

VIDF exhibits peak during the melting transition and hence the melting point can be determined effectively.

- **Mean squared displacement :** Mathematically, the Mean Squared Displacement (MSD) is defined as :

$$MSD(t) = \frac{1}{N\tau_{max}} \sum_{\tau=1}^{\tau_{max}} \sum_{j=1}^{N} \Big[\mathbf{r}_j(t+\tau) - \mathbf{r}_j(\tau) \Big]^2. \tag{1.56}$$

where, τ_{max} denotes the number of time origins over which averaging has been performed and t denotes delay time. In case of normal diffusion MSD scales linearly with time whereas, in case of anomalous diffusion MSD scales either more rapidly (superdiffusion) or less rapidly (subdiffusion) with time.

- **Velocity Auto Correlation Function :** The Velocity Auto Correlation Function (VACF) is defined as :

$$VACF(t) = \frac{1}{N\tau_{max}} \sum_{\tau=1}^{\tau_{max}} \sum_{j=1}^{N} \mathbf{v}_j(t+\tau) \cdot \mathbf{v}_j(\tau), \tag{1.57}$$

where, τ_{max} denotes the number of time origins over which averaging has been performed and t denotes delay time. The VACF provides valuable information about the dynamics and transport properties of a many particle system. Specifically, the long time behaviour of VACF can be related to the diffusion coefficient of the particles. It also provides insights about the collective modes and oscillations in a system.

1.13 Scope of this thesis

In the remainder of this thesis, we explore the static structure, collective dynamics, single particle dynamics and phase transition of finite dust clusters in complex plasma. To study these aspects, we have employed several diagnostic measures as given in the previous section. First, we investigated the effect of dust-neutral collision on the static structure and dynamic properties of a three-dimensional Yukawa cluster. We compared observations from frictionless Molecular Dynamics (fMD) and Langevin Dynamics (LD) simulations to better understand the effect of dust-neutral collision on the static structure and dynamic properties of the cluster. Secondly, we studied the effect of applying an external magnetic field in the cluster dynamics in the absence of dust-neutral collision. This introduces an additional time scale into the system, namely the Cyclotron time scale. It has been shown that at a sufficiently strong magnetic field and large value of coupling strength, the system of particles exhibits ordered rotational motion in contrast to disordered rotational motion at lower values of magnetic field strength and coupling strength. The phase transition from ordered to disordered rotational motion was identified as a first order phase transition. This gives us a phase boundary dividing the magnetic field - temperature plane into two distinct time scale regimes. Thirdly, we explored the effect of a transverse external magnetic field in the collective and single particle dynamics of a two dimensional Yukawa cluster in complex plasma. It was found that the dominance of cyclotron time

scale over dust-dust interaction time scale and harmonic confinement time scale can lead to some intriguing collective and single particle phenomena. Specifically, as the cyclotron frequency becomes larger than the dust plasma frequency, the phonon spectra splits up and for very high value of cycltron frequency the higher frequency branch was found to approach cyclotron frequency. In case of single particle dynamics, as the cyclotron frequency exceeds the harmonic frequency the cluster was found to cross over from normal to a superdiffsive regime.